Structure of oriented V_2O_5 gel studied by polarized x-ray-absorption spectroscopy at the vanadium K edge

S. Stizza and G. Mancini
Dipartimento di Matematica e Fisica, Università di Camerino, I-62032 Camerino, Italy

M. Benfatto and C. R. Natoli
Instituto Nazionale di Fisica Nucleare, Laboratori Nazionali di Frascati, I-00044 Frascati, Italy

J. Garcia
Instituto de Ciencia de Materiales de Aragon, Consejo Superior de Investigaciones Científicas, Universidad de Zaragoza, 50009 Zaragoza, Spain

A. Bianconi
Dipartimento di Fisica, Università di Roma, "La Sapienza," I-00185 Roma, Italy
(Received 15 March 1989; revised manuscript received 24 July 1989)

The local structure around the vanadium site in the oriented $V_2O_5 \cdot 1.6\ H_2O$ dehydrated xerogel phase is investigated by polarized x-ray-absorption spectroscopy (XAS). A large dychroism is found both in the extended x-ray-absorption fine structure (EXAFS) and in x-ray-absorption near-edge structure (XANES). A joint analysis of EXAFS and XANES data is reported. EXAFS analysis has been performed using a spherical-wave propagator and XANES analysis by full multiple-scattering calculation. A detailed discussion about the origin of all the different features in the experimental XAS spectra and a method to extract small contributions in the EXAFS part of the spectrum is presented. Moreover, the local structure around the vanadium atom in the V_2O_5 hydrogel phase is derived.

I. INTRODUCTION

The coordination chemistry of vanadium in V_2O_5 oxides is an interesting problem in relation to its physical chemical properties for the different, aggregate states. Its semiconducting properties in amorphous glasses[1] and catalyst properties in the selective oxidation of hydrocarbons[2] are indeed well known.

The vanadium pentoxide can be also found in a gel state which exhibits very interesting properties, such as, for example, the electrical conductivity which is about 3 orders of magnitude higher than that of crystalline V_2O_5 oxide. This fact, together with the easy manipulation of this compound, could open new applications in technology and material science. It is evident that an interpretation of any type of properties of these compounds cannot be pushed forward without a knowledge of their geometrical structure. A great amount of study has been focused in this direction by using electron, x-ray, and neutron diffraction[3–5] for a V_2O_5 solid-phase gel with an approximate formula $V_2O_5 \cdot 1.6\ H_2O$ (xerogel phase). On the basis of these experiments, the vanadium pentoxide xerogel, obtained by spontaneous dehydration at room temperature of V_2O_5 hydrogel, is thought to be formed by layers of oriented pyramids. Their bases are formed by a distorted square plane and linked in such a way to form layers separated by water molecules. The interlayer spacing is about 11.5 Å. The vanadium site structure in a V_2O_5 crystal is formed by four oxygen atoms at the corner of the basis of a distorted pyramid and one oxygen atom at the top with a very short bond length of about 1.58 Å (in the following we refer to this direction as z axis). There is another oxygen below the basis of the pyramid with a longer bond distance of about 2.7 Å which belongs to the adjacent vanadium cluster.[6] In the dehydrated xerogel compound, the geometrical arrangement around the vanadium atom is quite similar, but the long oxygen below the basis belongs now to a water molecule. The geometrical structure is reported in Fig. 1. For the sake of clarity the bases of the pyramids are depicted as squares.

The aim of this paper is to contribute to a better knowledge of the structure of this compound by means of x-ray-absorption spectroscopy (XAS). An explanation of the well-known "dark" XAS spectrum[7] of the vanadium pentoxide compounds is given. Both x-ray-absorption near-edge structure (XANES) and extended x-ray-absorption fine-structure (EXAFS) parts of the spectrum at the vanadium K edge are in fact investigated.

X-ray-absorption spectroscopy gives a unique probe for the local structure determination around the photoabsorber[8] due to the strong interaction of the photoelectron with the environment. Moreover, the linear polarization characteristic of the synchrotron radiation allows us to perform polarized experiments in anisotropic systems as in the case of the dehydrated V_2O_5 xerogel oriented phase. The analysis of the unpolarized XAS spectra of the V_2O_5 compounds presents severe difficulties both in

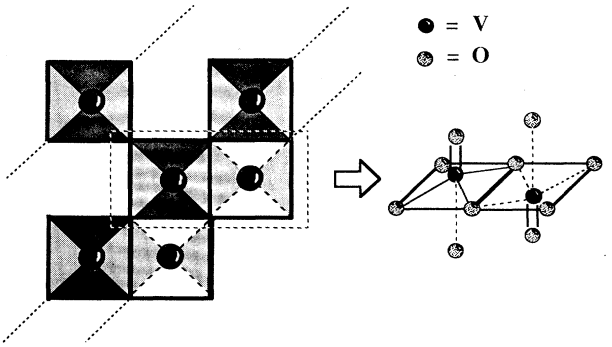

FIG. 1. Schematic picture of the $V_2O_5 \cdot 1.6\ H_2O$ xerogel phase structure. In the left part of the figure the projection on the layer plane of the three-dimensional structure is depicted. Each unit represents a vanadium-oxygen pyramid. The different characterization of the units indicates a different orientation of the pyramids. A detailed view of the local structure is given in the right part of the figure.

the XANES and EXAFS part. Concerning the EXAFS energy region, it is well known[9] that the spread of the vanadium oxygen distances in the first coordination shell is such that a destructive interference occurs between different contributions. In practice, due to the limited measured energy range and the rapid decrease of the backscattering amplitude of the oxygen, it is impossible to separate the different distances by a conventional "Fourier-transform" analysis. For these reasons it is necessary to extend the EXAFS analysis at the low-k domain and to use polarized spectra in order to select particular V-O paths to separate the signal coming from different atoms. Regarding the XANES part of the spectrum, the main difficulty lies in the fact that it is impossible to assign the experimental features to a particular geometrical structure.

Dramatic changes are observed in the experimental spectra by changing the angle between the electric field vector **E** and the layer plane.[9] This is a clear indication that the pyramids are well oriented. Due to this orientation, in the high-k ($\gtrsim 5$ Å^{-1}) region of the EXAFS signal when the electric field **E** is on the layer plane, the main contributions come only from the atoms on this plane whereas when the electric field **E** is parallel to the z axis, the main contributions come from atoms along this direction. In the XANES region it is impossible to separate so well the contributions coming from different directions due to the curved-wave nature of the photoelectron wave,[10] but the possibility of collecting different spectra for different polarizations allows the assignment of the various experimental features to definite geometrical structures.

The paper is organized as follows. Section II is devoted to the experimental details, while the theoretical background, based on the multiple-scattering (MS) theory, is reported in Sec. III. Section IV contains the XANES analysis of the two different polarized experimental spectra. This analysis is based on a series of different MS calculations obtained by changing the geometrical environment around the photoabsorber for the two different polarizations. In such a way the experimental features are assigned to a particular geometrical environment. The EXAFS analysis is reported in Sec. V. The main characteristic of this analysis is the use of curved-wave propagators to go to the low-k domain and a subtraction procedure already used[11] to extract small signals. The last section of the paper is devoted to the conclusions.

II. EXPERIMENTAL

A thin film of V_2O_5 dehydrated xerogel was obtained by spontaneous evaporation of the solution on a Mylar thin window. The vanadium pentoxide layers lie in the mylar plane. The surface was taken about 10×20 mm^2. The polarized EXAFS and XANES spectra were taken at the Frascati Radiation Facility using the storage ring ADONE working at 1.5 GeV with a current of about 50 mA. Monochromatization was obtained by a double-channel cut Si single crystal working at the (111) reflection. The spectra were measured in the transmission mode in such a way that when our sample was perpendicular to the beam, the electric field **E** was in the layer plane. During the measurements the samples were kept in a vacuum chamber with a pressure of about 10^{-4} Torr. To change the polarization, we simply rotated the sample around the axis that lies in the sample plane and is perpendicular to the plane of the electronic orbit. Spectra at angles $\alpha = 20°$, 30°, 50°, 70°, and 90° (α being the angle formed between the electric field **E** and the z axis) were recorded.[9] The XANES spectra of the hydrogel phase have also been recorded using a Mylar cell 1 mm thick. The 0° polarization spectrum, which is not measurable directly, has been obtained taking the correct linear combination between the spectra with $\alpha = 20°$ and 90°. The experimental polarized XANES and EXAFS spectra of V_2O_5 xerogel, after normalization, are reported in Figs. 2(a) and 2(b), for the electric field **E** perpendicular (xy polarization) and parallel (z polarization) to the **z**

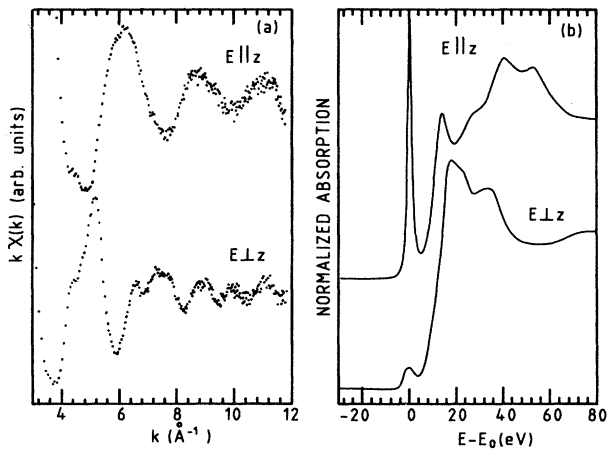

FIG. 2. (a) Experimental EXAFS spectra of the V_2O_5 xerogel at the K edge of vanadium for the electric field perpendicular and parallel to the layer plane. (b) Normalized XANES spectra of the V_2O_5 xerogel for both polarizations.

axis. The main characteristic of the z-polarized spectrum is the presence of a well-defined preedge structure due to the $1s \rightarrow 3d$ transition. The intensity of this transition is a function of the angle α and goes to zero for $\alpha = 90°$. The small preedge feature that remains for $\alpha = 90°$ is due to a slight misalignment of the sample with respect to the x-ray beam,

At first sight, the EXAFS spectrum for z polarization shows a nearly single oscillation, while the one for xy polarization shows a multiple structure with several oscillatory contributions due to different atoms in the layer plane.

III. THEORETICAL CALCULATION

In the multiple-scattering theory the x-ray-absorption coefficient for photons of frequency ω and polarization vector ε due to the excitation of a core level of atoms of density N_c can be written in atomic units as[12,13]

$$\mu_c = N_c \sigma(k;\varepsilon) = N_c 4\pi\omega\alpha k \,\mathrm{Im}\left[\sum_{i,L,L'} (i|\mathbf{r}\cdot\boldsymbol{\varepsilon}|R_l Y_L)\tau^{00}_{LL'} \times (R_{l'} Y_{L'}|\mathbf{r}\cdot\boldsymbol{\varepsilon}|i)\right], \tag{1}$$

where k is the wave vector of the photoelectron, α is the fine-structure constant, and the spin dependence has been neglected. The R_1's are regular solutions of the radial Schrödinger equation in the photoabsorber muffin-tin (MT) sphere matching to

$$R_l \approx j_l \cos\delta_l - n_l \sin\delta_l$$

at the muffin-tin radius, where j_l and n_l are spherical Bessel and Neumann functions and δ_l is the MT potential lth phase shift. All the structural information is contained in the quantity

$$\tau^{00}_{LL'} = \frac{1}{\sin\delta^0_l}\frac{1}{\sin\delta^0_{l'}}[(T_a^{-1} - G)^{-1}]^{00}_{LL'}, \tag{2}$$

where δ^0_l is the l-phase shift of the absorbing atom, assumed located at site 0, $G \equiv G_{LL'}$ is the matrix describing the free spherical-wave propagation of the photoelectron from site i and angular momentum $L = (l,m)$ to site j and angular momentum $L' = (l',m')$ in the angular momentum representation, and $T_a \equiv \delta_{ij}\delta_{LL'}[\exp(i\delta^i_l)\sin\delta^i_l]$ is the diagonal matrix of atomic t-matrix elements describing the scattering process of the L spherical-wave photoelectron by the atom located at site i with phase shift δ^i_l. Under certain conditions (we refer to Ref. 13 for a complete discussion) it is possible to express the structural factor as an absolutely convergent series relative to some matrix norm and to expand the photoabsorption cross section $\sigma(k;\varepsilon)$ in partial contributions as follows:

$$\sigma(k;\varepsilon) = \sum_{n=0} \sigma_n(k;\varepsilon), \tag{3}$$

where $\sigma_0(k;\varepsilon)$ is a smooth atomic-absorption cross section and each contribution $\sigma_n(k;\varepsilon)$ of order n represents all processes where the photoelectron emanating from the photoabsorber is scattered $n-1$ times by the surrounding atoms before returning to it. Clearly these quantities are related to the n-particle correlation function.[11,14] In particular the $\sigma_2(k;\varepsilon)$ is the EXAFS term in the spherical-wave representation which can be written for the K edge as[10]

$$\sigma_2(k;\varepsilon) = -|M_{01}(k)|^2 \sum_j \mathrm{Im}\left[\frac{e^{2i(\rho_j + \delta^0_l)}}{\rho_j^2}\sum_l (-1)^l(2l+1)t^J_l[\cos^2\theta_j (g^{(0)}_{1l})^2 + \sin^2\theta_j (g^{(1)}_{1l})^2]\right], \tag{4}$$

where $\rho_j = kR_j$, θ_j is the angle between the polarization vector ε and the direction R_j joining the jth atom with the absorbing one, $|M_{01}(k)|^2$ is the radial matrix element between the initial $l=0$ state and the final dipole allowed R_1 radial wave function, and[10]

$$g^{(0)}_{1l} = \frac{(l+1)C_{l+1}(\rho) + lC_{l-1}(\rho)}{2l+1},$$

$$g^{(1)}_{1l} = \left[\frac{l(l+1)}{2}\right]^{1/2}\frac{C_{l+1}(\rho) - C_{l-1}(\rho)}{2l+1}.$$

The quantity C_l can be written in terms of Hankel functions as

$$C_l = i^{l+1}\rho e^{-i\rho} h_l^+(\rho).$$

The presence of the term proportional to $\sin^2\theta$ has two main implications: first, the amplitude and the phase functions in the EXAFS signal are angle dependent, and secondly, there are contributions from atoms with bonds perpendicular to the electric field. As discussed in Ref. 10 the $\sin^2\theta$ term is associated with the high-l components in the l sum of Eq. (4) and its strength is strongly system dependent. In our case we have verified that the magnitude of the corrections associated to the $\sin^2\theta$ term is negligible in the phase function and never exceeds 1% in the amplitude function in the whole energy range.

To evaluate the atomic phase shifts we have used the $Z+1$ approximation for the potential in the final state with the ordinary $X\alpha$ energy-independent exchange and the usual Mattheiss prescription for the muffin-tin approximation.

In the following we refer to Eq. (1) for the total XANES calculation, where all MS contributions are included, and to Eq. (4) for the EXAFS analysis. In this last case, thermal disorder and inelastic losses are included in the usual way.[8]

IV. XANES ANALYSIS

In order to obtain the structural information from XANES spectra, several model calculations have been performed. All the calculations were made by approximating the real cluster of atoms around the photoabsorber with C_{4v} and C_{2v} geometries. In Fig. 3 the comparison between the experimental spectra related to the two different polarizations and a set of several calculations is shown. In order to determine the origin of the experimental features in the spectra, model calculations have been performed beginning with the simplest: model *a*. In this model only the first coordination shell of oxygen atoms is taken into account. The cluster has C_{4v} symmetry and the vanadium atom is surrounded by a pyramid of oxygen atoms. There is one oxygen in the *z* direction at 1.58 Å and four oxygens in the square basis at 1.87 Å. The vanadium atom is displaced out of the square plane by 0.25 Å. The calculation made using this model accounts for the main shape observed in the *xy*-polarized spectrum. On the contrary the *z*-polarized calculation reproduces the preedge feature rather well, but does not account for the details present in the experimental spectrum. The sharp preedge feature is assigned to the transition to any empty antibonding state formed by the $2p$ orbitals of the shortest oxygen and the $3d$ orbitals of the vanadium. Approximating the real cluster with C_{4v} symmetry, this feature comes from the transition to a state belonging to the A_1 representation of the C_{4v} point group which can be reached only with light polarized in the *z* direction. The states belonging to the E_1 representation are deeper in energy and completely occupied. In fact, no asymmetry is observed in the experimental preedge feature. This is the reason for the absence of a similar structure in the other polarization. Moreover, this finding rules out other local point symmetries of higher order like the tetrahedral one.[15]

In order to give a better description of the details observed in the experimental *z*-polarized spectrum, we have calculated a little more complicated geometrical cluster following two ideas. First, the square oxygen base has been distorted to a rhombic shape which is a better approximation of the real V_2O_5 crystal geometry. Secondly, another oxygen has been added below the oxygen plane in order to account for the richness of features obtained in

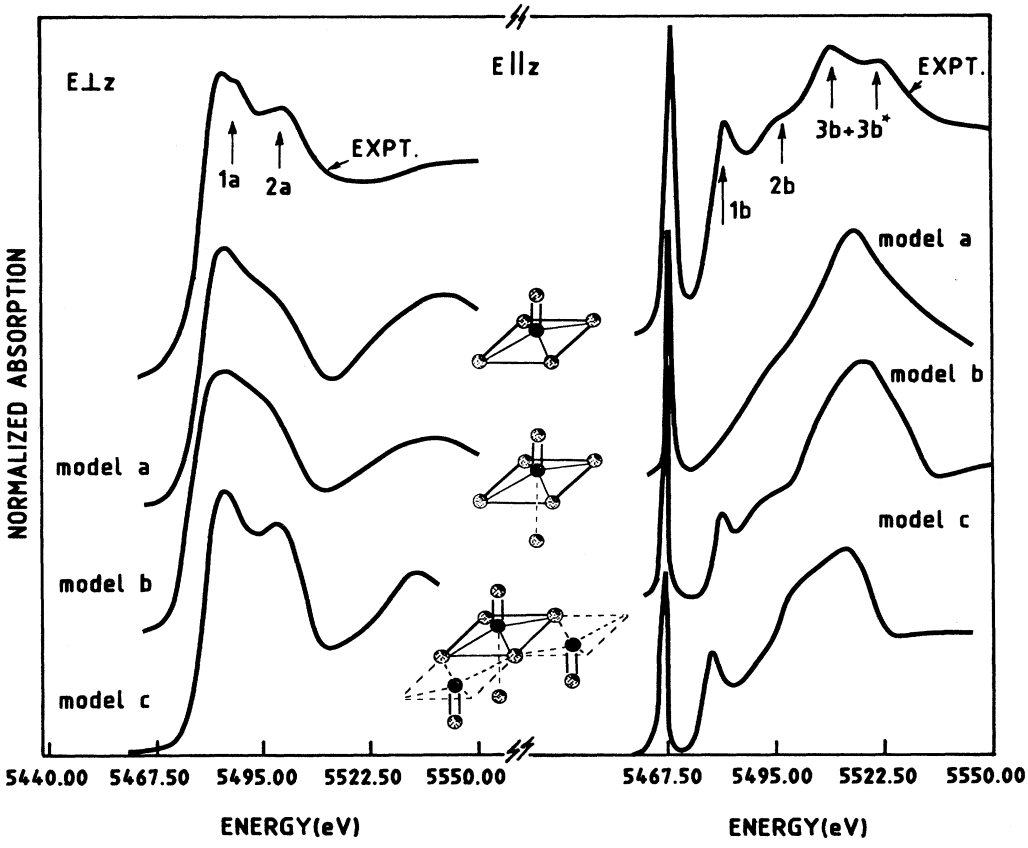

FIG. 3. Comparison between the experimental XANES of xerogel phase in the two polarizations and a set of different calculations made using the clusters indicated in the insets and described in the text. The main experimental features are indicated by arrows in the figure. A complete discussion about the origin of these structures is given in the Sec. IV of the text.

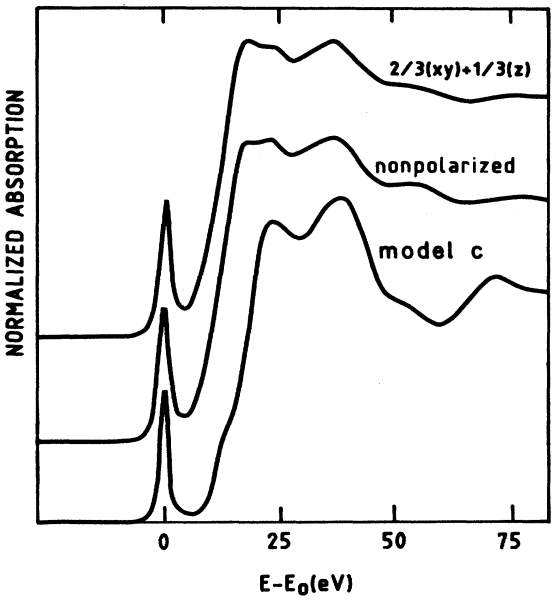

FIG. 4. Comparison among the linear combination of $\frac{1}{3}$-z polarized plus $\frac{2}{3}$-xy-polarized spectra of xerogel phase (uppermost curve), the nonpolarized experimental XANES spectrum of hydrogel phase, and the total calculation obtained by using model c depicted in the previous figure and discussed in the text.

the z polarization. In fact, the structure in the z polarization mainly derives from MS processes involving interatomic pathways lying in the z direction. This oxygen simulates the presence of water molecules between the layers which are weakly linked to the vanadium atom. This new cluster, called model b in Fig. 3 now has C_{2v} symmetry. The V-O distances in the rhombic base are 2.10 and 1.76 Å and the oxygen below the plane is at 2.7 Å far from vanadium atom as in crystalline V_2O_5. All the other distances are the same as in the previous model. The **xy**-polarized calculated spectrum remain essentially unchanged, while in the **z**-polarized spectrum, the presence of features $1b$ and $2b$ can be observed, in agreement with the experimental result, although the energy separation between the two features is not well reproduced. But, the presence of features $1b$ and $2b$ clearly indicates the presence of the water molecules below the plane. Other calculations, not reported here for simplicity, confirm this interpretation.[16]

Finally, the last calculation, model c in Fig. 3, was made on the basis of the "naive" consideration that the **xy**-polarized EXAFS results are formed by several oscillatory contributions and on the basis of the more precise EXAFS results presented in the next section. This new cluster is the same as model b with four more atoms. These latter atoms are the vanadium atoms in the second shell (V-V distance is 3.08 Å) together with their shortest oxygens as clearly depicted in the sketch of Fig. 3. The effect of including these new atoms in the calculation is important especially for the xy polarization, where the features $1a$ and $2a$ are now rather in agreement with the experimental result both in intensity and energy position. In the other polarization, the effect is weak but the shape of the calculated spectrum is now in better agreement with the experimental result. The energy separation between the features $1b$, $2b$, and $3b$ is reasonably well reproduced considering that the charge-density distribution of the model cluster is not self-consistent, but feature $3b^*$ is absent. Other calculations, which are not reported in this paper for simplicity, made using more complicated clusters do not improve the agreement between the experimental and the theoretical results. This fact is not surprising because neither disorder (thermal and structural) at all nor inelastic losses have been considered in the calculations. It is also possible that feature $3b^*$ be a multielectron excitation.[17]

In Fig. 4 the comparison among the experimental spectrum of the hydrogel solution, the sum $\frac{2}{3}(xy)+\frac{1}{3}(z)$ of the xerogel experimental spectra, and the theoretical calculation made on the basis of model c is reported. From this comparison it is clear that the xerogel and hydrogel phases of the V_2O_5 compound have the same geometrical structure around the vanadium photoabsorber. Moreover, the difficulties in analyzing the experimental spectrum of the nonpolarized V_2O_5 compounds can be overcome by the separate study of the two different polarizations.

With these considerations in mind, we can fix the basic geometrical configuration of the vanadium site as formed by a bipyramid of oxygen atoms in the first shell and some vanadium atoms in the second shell belonging to the adjacent bipyramids.

V. EXAFS ANALYSIS

Following the qualitative XANES analysis, we have performed a detailed analysis of the EXAFS spectra.

The EXAFS signal for the z polarization, reported in Fig. 5(a), is dominated by a single main oscillation coming from the shortest oxygen atom perpendicular to the basis of the pyramid. The modulus of the Fourier transform of this signal [Fig. 5(b) dotted line] gives a main peak indicating a single coordination shell. Looking carefully at this experimental Fourier transform (FT) more structure can be observed in the range between 2.4 and 4.0 Å which is difficult to separate from the experimental noise. In order to determine if this guess is correct, a minimum square fit of the experimental signal is made using just one oxygen atom with theoretical phase shifts coming from the model c (see XANES section) and the spherical-wave propagator [see Eq. (4)]. For simplicity, due to the smallness of the correction associated to the $\sin^2\theta$ term, we have neglected this contribution in our EXAFS calculations and fits. The best fit gives for this shell the following parameters: vanadium-oxygen distance $R=1.58$ Å, coordination number $N_1=1$, and Debye-Waller factor $\sigma^2=0.002$ Å^2. In Fig. 5(a) the comparison between the signal coming from this fit (solid line) and the experimental spectrum is also reported. Although the main oscillation is well reproduced, slight discrepancies are present, especially in the low-k domain. The comparison between the FT of the experimental signal and the theoretical one confirms this indication [Fig. 5(b) solid line]. Indeed the small structure present in the

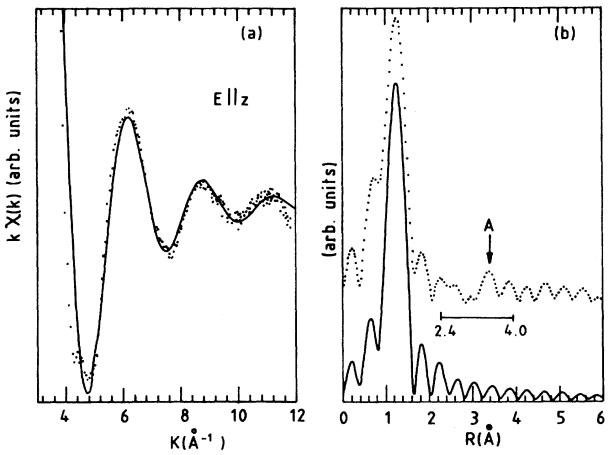

FIG. 5. (a) Experimental $kX(k)$ oscillation for $E\|z$ (dotted line) and theoretical fitting using one shell with only one oxygen atom. (b) Modulus of the Fourier transforms of the experimental and theoretical $k^3X(k)$ signals taken in the range $3.7 \leq k \leq 11.8$ Å^{-1} using a 0.2-Å^{-1} Hanning window. The range between 2.4 and 4.0 Å is underlined. Arrow A indicates the contribution of the shortest oxygens belonging to adjacent pyramids.

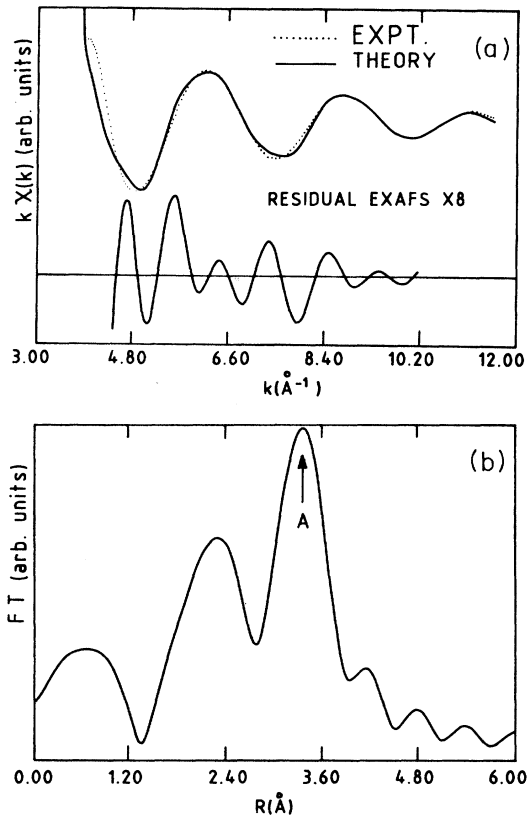

FIG. 6. (a) In the upper part are compared the Fourier-filtered experimental spectrum for $E\|z$ polarization (dotted line) with the theoretical fitted spectrum using one oxygen as back-scattering atom. The lower curve (residual part) is the difference between the two spectra. The vertical scale of this residual signal is eight times greater than the full spectrum. (b) Modulus of the Fourier transform of the residual signal. Arrow A indicates the same contribution as discussed in the previous figure.

experimental FT in the 2.4–4.0-Å range is absent in the theoretical FT, indicating the presence of weak contributions (the main one is indicated as A in the figure) due to other shells. In order to extract these contributions, we have performed the analysis following a subtraction procedure already used to single out MS contributions in other compounds.[11] First, the experimental signal was filtered by a FT technique, where the back-Fourier-transform was taken between 0.9 and 4.0 Å. The spectrum so obtained reproduces the nonfiltered EXAFS signal well, showing that all the physical contributions are in this range. Then, from this spectrum the theoretical EXAFS, calculated using Eq. (4) of the text, due to the shortest oxygen was subtracted, obtaining a residual signal. The whole procedure is indicated in the upper part of Fig. 6 where back-Fourier, theoretical EXAFS and difference signals are reported. The residual represents less than 9% of the total EXAFS in this direction, and its FT is reported in Fig. 6(b). Two peaks at 2.3 and 3.4 Å are observed. The first one at 2.3 Å may be assigned to the presence of a water molecule below the basis of the vanadium pyramid at a distance of 2.7 Å as in crystalline structure and in agreement with the XANES analysis made in the previous section, while the second peak at 3.4 Å (peak A in the figure) is due to the shortest oxygen atom in the adjacent vanadium pyramid which is at a distance of about 3.7 Å. Following this interpretation, the experimental spectrum has been fitted using three coordination shells. In Fig. 7 the comparison between the filtered experimental signal and the theoretical one so obtained is reported. The agreement is quite good. In the same figure the residual signal which is quite structureless is also reported, showing that all the physical contributions in the EXAFS have been extracted. The fitting pro-

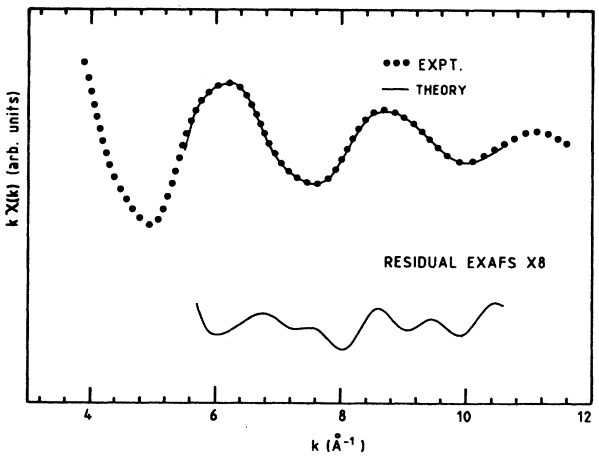

FIG. 7. Experimental Fourier-filtered EXAFS spectrum for $E\|z$ polarization (dotted line) compared with theoretical fitting using the shells described in the text. The lower curve is the difference between the two upper curves. The vertical scale of the residual part is multiplied by eight.

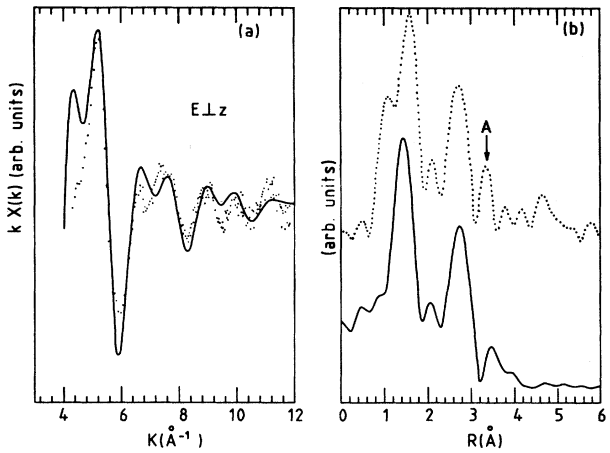

FIG. 8. (a) Comparison between the EXAFS experimental spectrum for $E\|xy$ polarization (dotted line) and theoretical fitting using a first shell of four oxygen atoms at the crystallographic distances and a second shell formed by two vanadium atoms at 3.2 Å and two oxygens at 3.7 Å (solid line) as described in the text. (b) Modulus of the Fourier transform of the experimental EXAFS spectrum (upper curve) and of the theoretical simulation (lower curve). Peak A has the same meaning of the one discussed in the caption of Fig. 5.

cedure gives for the first shell the same parameters reported above, for the second shell a V-O distance at 2.7 Å with a big Debye-Waller factor $\sigma^2=0.010$ Å^2, and a coordination number $N=0.58$, and for the third shell a V-O distance of 3.7 Å, a Debye-Waller factor $\sigma^2=0.008$ Å^2, and an effective coordination number $N_{\text{eff}}=0.63$. From these results, it is clear that the water molecules are weakly linked to the vanadium atoms. Moreover, since the angle between the electric field and the vector joining the photoabsorber and the oxygen in third shell is about $\theta=35°$, the real coordination number is $N_3=0.63/\cos^2 35°\approx 1.88$ which gives at least two adjacent pyramids in the edge-sharing mode relative to the central one containing the photoabsorber.

The EXAFS signal for E⊥z [Fig. 8(a)] is clearly much more structured than the one for the other polarization indicating strong contributions from shells further away than the first one. In Fig. 8(b) (dotted line) is reported the FT of this signal which confirms such an indication. Two main peaks can be observed; the first one at 1.56 Å comes from the four oxygen atoms in the basal plane of the pyramid, while the second one at 2.75 Å comes from the vanadium atoms which belong to the adjacent pyramids. Peak A comes from the shortest oxygen atom belonging to the adjacent vanadium pyramid. In Fig. 8(a) the comparison between the experimental signal and the theoretical EXAFS obtained by using four oxygens at the crystallographic distances in the first shell, two vanadium atoms at a distance of 3.08 Å, and two oxygens at 3.70 Å, which are the shortest oxygens belonging to the adjacent pyramids in the second shell is reported. The FT of this theoretical signal is reported in the lower curve of Fig. 8(b) (solid line). The agreement between the theoretical and the experimental signal is rather good, and the discrepancies might be due to the fact that we do not take into account the structural disorder of the atoms belonging to higher-order shells.

To conclude this section we observe that the presence of peak A in all experimental FT's confirms the fact that this structure is due to the shortest oxygens which belong to the adjacent pyramids as described above. Indeed, the angle between the electric field and the vector joining the photoabsorber and this oxygen atom is 35° when the field **E** is parallel to the z axis, while this oxygen atom is 55° when the field **E** is perpendicular to the z axis.

VI. CONCLUSION

In this work we have studied the XANES and EXAFS spectra for electric field parallel and perpendicular to the pyramidal basal plane at the K edge of the vanadium in the V_2O_5 gel. It turns out from this analysis that the V_2O_5 gel is formed by layers of well-oriented pyramids. The local structure around the vanadium atoms is quite similar to that in V_2O_5 crystal, but the oxygen atom below the pyramidal base belongs now to the water molecules between layers. Both XANES and EXAFS analyses indicate that the edge-sharing pyramids are flipped upside down as shown schematically in Fig. 1. These results substantially confirm the geometrical structure of the V_2O_5 xerogel compound derived by other experimental techniques.[3–5] Another important result is that the hydrogel and xerogel have the same local structure around the vanadium site. Moreover, the possibility of studying separately the XANES and EXAFS spectra related to the two different polarizations has allowed us to assign all the features in the experimental spectra of V_2O_5 compounds to a specific geometrical structure.

From the previous discussion a useful method of analysis of a XAS spectrum to obtain structural information can be derived. Generally speaking one can distinguish three energy regions in a photoabsorption spectrum: a full multiple-scattering (FMS) region, where numerous or an infinite number of scattering terms [see Eq. (3) of Sec. III] of high order contribute to the final shape, followed by a intermediate multiple-scattering (IMS) energy region where only few terms of low order are important, this region merging continuously into the single-scattering (SS) regime. Normally for low Z scatterers the SS terms dominate above wave-vector values of $k\geq 4$ Å^{-1}, but the energy extent of each region is strongly system dependent. In the FMS region only a comparison between the experimental signal and a theoretical calculation obtained by Eqs. (1) and (2), and related to a given structural model can be safely used due to the great or infinite number of terms needed to reconstruct the shape of the experimental spectrum. In this way only global structural information can be obtained. On the contrary in the IMS and SS region the absorbing coefficient is formed by superposition of few different signals related to various MS and/or SS contributions according to the associated paths. Each signal has the same sinusoidal behavior with different periods and phases. The main contributions can be theoretically calculated or

experimentally derived and subsequently subtracted from the total to single out small contributions of MS and/or SS type. A combination of FT and fitting techniques can be used to analyze such contributions. In the present case the IMS region seems to be missing, probably due to the washing effect of the compositional disorder on an already small MS signal. Therefore, we have limited our analysis to the FMS and the SS regions.

Another possibility is to fit all the signals present in the spectrum by the same sinusoidal type of function having different period and phases according to the length and the type of the associated path. In this way the inaccuracies of the subtraction procedure can be avoided. This last procedure has been recently proposed to analyze the three-body correlation function in amorphous silicon.[18]

To summarize a twofold goal has been achieved. First, the local geometrical structure around the vanadium of xerogel and hydrogel V_2O_5 compounds has been resolved, and second a viable method of analysis of a XAS spectrum has been proposed that combines the advantages of both FT and fitting techniques.

ACKNOWLEDGMENTS

We want to thank Professor J. Livage for providing us with the xerogel samples and for several illuminating discussions. This work has been partially supported by the cooperation agreement between La Comisión Asesora de Investigación Científica y Técnica (CAICYT) (Spain) and Instituto Nazionale di Fisica Nucleare (Italy) (INFN).

[1]A. Mosset, P. Lecante, J. Galy, and J. Livage, Philos. Mag. B **46**, 137 (1982).
[2]M. S. Wainwright and N. R. Foster, Catal. Rev. **19**, 211 (1979).
[3]J. J. Legendre and J. Livage, J. Colloid Interface Sci. **94**, 75 (1983).
[4]J. J. Legendre, P. Aldebert, N. Baffier, and J. Livage, J. Colloid Interface Sci. **94**, 84 (1983).
[5]P. Aldebert, H. W. Haesslin, and J. Livage, J. Colloid Interface Sci. **98**, 478 (1983); **98**, 484 (1983).
[6]H. G. Bachman, F. R. Ahmed, and W. H. Barnes, Z. Kristallogr. **115**, 110 (1961).
[7]R. Kozlowski, R. F. Pettifer, and J. M. Thomas, J. Phys. Chem. **87**, 5176 (1983).
[8]For a review see, EXAFS and Near Edge Structure IV, edited by P. Lagarde, D. Raoux, and J. Petiau [J. Phys. (Paris) Colloq. **47**, C8-691 (1986)].
[9]S. Stizza, M. Benfatto, A. Bianconi, J. Garcia, A. Mancini, and C. R. Natoli, J. Phys. (Paris) Colloq. **47**, C8-691 (1986).
[10]M. Benfatto, C. R. Natoli, C. Brouder, R. F. Pettifer, and M. F. Ruiz-Lopez, Phys. Rev. B **39**, 1936 (1989).
[11]M. Benfatto, C. R. Natoli, A. Bianconi, J. Garcia, A. Marcelli, M. Fonfoni, and I. Davoli, Phys. Rev. B **34**, 5774 (1986).
[12]W. L. Schaich, Phys. Rev. B **29**, 6513 (1984).
[13]C. R. Natoli and M. Benfatto, J. Phys. (Paris) Colloq. **47**, C8-11 (1986).
[14]M. Benfatto, C. R. Natoli, J. Garcia, and A. Bianconi, J. Phys. (Paris) Colloq. **47**, C8-25 (1986).
[15]A. Bianconi, J. Garcia, and M. Benfatto, in *Synchrotron Radiation in Chemistry and Biology I,* edited by E. Mandelkow (Springer-Verlag, Berlin, 1988).
[16]M. Benfatto and J. Garcia (unpublished).
[17]A. Bianconi, J. Garcia, M. Benfatto, A. Marcelli, C. R. Natoli, and M. F. Ruiz-Lopez, Phys. Rev. B (to be published).
[18]A. Filiponi, A. Di Cicco, M. Benfatto, and C. R. Natoli (unpublished).

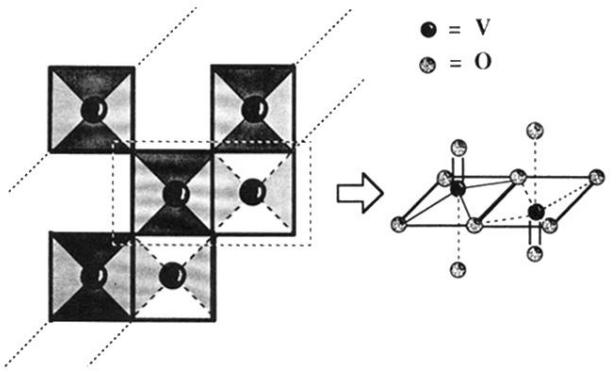

FIG. 1. Schematic picture of the $V_2O_5 \cdot 1.6\ H_2O$ xerogel phase structure. In the left part of the figure the projection on the layer plane of the three-dimensional structure is depicted. Each unit represents a vanadium-oxygen pyramid. The different characterization of the units indicates a different orientation of the pyramids. A detailed view of the local structure is given in the right part of the figure.